Powered Ankle-Foot Prosthesis

©PUNCHSTOCK

The Importance of Series and Parallel Motor Elasticity

BY SAMUEL K. AU
AND HUGH M. HERR

Digital Object Identifier 10.1109/MRA.2008.927697

The loss of a limb is a major disability. Unfortunately, today's prosthetic technology is a long way from realizing fully functioning artificial limb replacements. Although lower-extremity prostheses are currently better able to provide assistance than their upper-extremity counterparts, very basic locomotory problems still remain. For example, compared with intact persons, walking amputees require 10–60% more metabolic energy depending on walking speed, physical fitness level, cause of amputation, amputation level, and prosthetic intervention characteristics. Additionally, amputees walk at 11–40% slower self-selected gait speeds than do persons with intact limbs [1]–[7].

Such clinical problems may, in part, be attributed to today's prosthetic ankle-foot designs. Commercially available prostheses comprise spring structures that store and release elastic energy throughout each walking stance period [8], [9]. Because of their passive nature, such prostheses cannot generate more mechanical energy than is stored during each walking step. In distinction, the human ankle performs positive net work and has a greater peak power over the stance period, especially at moderate to fast walking speeds [10]–[14].

A transtibial amputee overcomes these energetic deficiencies by using hamstring muscles to aggressively extend the hip throughout early stance [15]. Hyperactivity in this muscle group causes an excessive flexor moment about the knee, which then has to be canceled by cocontracting knee extensors. Winter and Sienko [15] hypothesized that this increase in muscle cocontraction results in a relatively higher gait metabolism. Another mechanism for the increased metabolic rate of walking amputees may be due to the inability of conventional prostheses to provide sufficient positive power at terminal stance to limit heel strike losses of the adjacent leg [14]–[16].

Several engineering challenges hinder the development of a powered ankle-foot prosthesis [15], [19], [20]. With current actuator technology, it is challenging to build an ankle-foot prosthesis that matches the size and weight of the human ankle-foot complex but still provides sufficient stance-period work and instantaneous power output to propel an amputee. Ankle-foot mechanisms for humanoid robots are often too heavy or not sufficiently powerful to meet the human-like specifications required for a powered prosthesis [21], [22]. Furthermore, a powered prosthesis must be position- and impedance-controllable. Often, robotic ankle controllers follow preplanned kinematic trajectories during walking [21], [22], whereas the human ankle is believed to operate in impedance control mode during stance and position control mode during swing [12]–[14].

A critical objective in the field of prosthetic leg design is to advance a powered ankle prosthesis capable of mimicking the dynamics of the human ankle. Some recent work has focused on the development of quasipassive ankle-foot prostheses. Researchers have built prostheses that use active damping or spring-clutch mechanisms to allow automatic ankle angle adjustment for distinct ground surfaces [8],

1070-9932/08/$25.00©2008 IEEE

[23], [25], [26] or to allow for an improved metabolic walking economy [24]. As these devices do not include an actuator to actively plantar flex the ankle at the terminal stance, no net work is performed throughout each walking step, as is the case with the human ankle [10]–[14].

In 1998, Klute and colleagues [27] were the first to build a powered ankle-foot prosthesis capable of performing net positive work. Their device employed a pneumatic actuation strategy with an off-board power supply. More recent work has focused on the design of energetically autonomous powered systems [28]–[36]. In this article, we review and further develop the ankle-foot design described in [28]–[35]. The article is organized as follows. In the next section, we present biomimetic design goals for the ankle-foot prosthesis, including prosthesis mass, torque, speed, bandwidth, net work, and stiffness. In subsequent sections, we discuss the importance of series and parallel motor elasticity in prosthesis shock tolerance, joint bandwidth, and energy economy. We conclude the article with the physical implementation of our design, including preliminary clinical data addressing the system's capacity to improve amputee gait.

Biomimetic Design Goals

We seek an ankle-foot prosthesis design that is capable of human-like ankle dynamics while still matching the shape and mass of the missing biological limb. Specifically, a biomimetic ankle-foot prosthesis should satisfy the following design specifications.

- *Size and mass*: Prosthesis height should be equal to or less than the nominal height of a conventional high-profile ankle-foot prosthesis, which is 18 cm from the ground to the proximal prosthetic adapter [8], [9]. The desired prosthesis mass should be 2.5% of the total body mass, which is equal to the percent mass of the missing biological limb at a point 18 cm from the ground surface [37].
- *Torque and speed*: The prosthesis should capture the entire torque-speed behavior of the human ankle in walking. The measured peak velocity, torque, and power of the human ankle during the stance period of walking can be as high as 3.6 ± 0.2 rad/s, 1.6 ± 0.2 Nm/kg, and 3 ± 1 W/kg, respectively. Here, both peak torque and power are normalized by body mass. These data are from [11], replotted in Figure 1 in the manner of [20].
- *Torque bandwidth*: The torque bandwidth requirement of the prosthesis was estimated based on the power spectrum of the human ankle torque data during the stance period of walking. The torque bandwidth was defined at that frequency range over which 70% of the total signal power was captured. Analyzing human ankle data from [11], the torque bandwidth was found to be approximately 3.5 Hz, at which the ankle torque varied between 50 and 140 Nm. The torque controller for the prosthesis should therefore be capable of outputting any torque level between 50 and 140 Nm at 3.5 Hz. This goal requires that the torque bandwidth of the open-loop system be significantly larger than 3.5 Hz, otherwise the inherent dynamics of the prosthesis may inhibit the controller's ability to specify the desired dynamics. Thus, an open-loop bandwidth is sought that is at least fivefold larger than the closed-loop bandwidth of 3.5 Hz.
- *Net positive work*: The prosthesis should also be capable of generating net positive work during stance. The average net positive work done at the human ankle per unit body mass for self-selected speed is 0.21 ± 0.05 J/kg [11].
- *Controlled dorsiflexion stiffness*: For the stance phase control, instead of simply tracking human ankle kinematics, it is commonly believed that a powered prosthesis should mimic the human ankle's quasistatic stiffness or the slope of the measured torque-angle curve during stance [12], [13]. Most critically, the prosthesis should output a human-like quasistatic stiffness during controlled dorsiflexion (or from point 2 to point 3 in Figure 1). A target stiffness value was obtained by estimating the slope of the measured human ankle torque-angle curve from the zero torque-angle point to the torque at maximum dorsiflexion (or point 3 in Figure 1). The average human ankle stiffness per unit body mass at a self-selected walking speed is 8 ± 1 Nm/rad/kg.

In this article, we design an ankle-foot prosthesis for a nominal male subject, walking at a self-selected speed of 1.25 m/s, whose body mass, height, and foot length are 78 kg, 175 cm, and 27 cm, respectively [40]. Table 1 lists the parameter values corresponding to the aforementioned design goals.

Shock Tolerance

Designing a motorized leg prosthesis that is robust to shock loads is a critical design challenge, especially at the most distal joint, or the ankle, where impact loads at foot strike have to be carefully managed. Series motor compliance [41]–[43] has been used in humanoid leg design [43] and leg exoskeletal applications [44]–[46] to effectively lower shock loads and protect the motor transmission from damage.

For a prosthetic ankle-foot device, how much series compliance is necessary to protect the transmission from excessive shock loads at heel strike? To answer this question, we employ a linear model of an ankle-foot prosthesis with a series elastic actuator (SEA) (see Figure 2). In the model, the effective mass M_e, linear motor force F_e, and damping b_e are defined as follows: $M_e = I_m R^2$; $F_e = T_m R$; and $b_e = b_m R$. The motor is modeled as a torque source T_m with a rotary internal inertia I_m, applying a force to the series spring k_s through a transmission R. State variables x and θ_m denote the linear and rotary motor displacements, respectively, where $x = \theta_m / R$. The damping term b_m represents motor friction from bearings and brushes. In the model, we assume that the foot is a rigid body of negligible mass, as foot mass is relatively small compared with the effective motor inertia. The equation of motion becomes

$$M_e \ddot{x} + b_e \dot{x} + k_s(x - \mathrm{r}\theta) = F_e. \tag{1}$$

This equation is the standard dynamic equation for an SEA [42], which ignores amplifier dynamics, nonlinear friction, and internal resonances. The series spring force $F_s = k_s(x - r\theta)$ acts at a perpendicular distance $\mathbf{r}$ from the ankle joint. Thus, ankle torque T_{ext} is equal to rF_s.

During the double support phase of nonamputee human walking, the trailing leg performs mostly positive external work on the body's center of mass, whereas the leading leg performs predominantly negative external work. In the human walking study of [47], the negative external work performed during double support was found to increase from 6.5 J at 0.75 m/s to 26.8 J at the maximum walking speed of 2.00 m/s. To determine the series stiffness k_s that adequately protects the transmission, we assume that the prosthesis worn on the leading leg has to absorb all 27 J of energy during ankle-controlled plantar flexion (see Figure 1). (This is a worst case condition since other joint motions are likely to contribute to negative external work production, such as early-stance knee flexion and subtalar joint inversion and eversion.) We simulate this condition by assuming that half the amputee's body mass (0.5 × 78 kg body mass) falls a distance of 7 cm from rest onto the linear SEA prosthesis of Figure 2(b). For this simulated heel strike, the amputee's body mass has 27 J of kinetic energy when the SEA ankle first begins to absorb energy at the instant of touch down. For this simulation, the peak shock load applied to the transmission is determined for each series stiffness value k_s. We assume that the ground reaction force acts at a point 3 cm posterior to the ankle rotational axis, as this is the approximate position of the center of pressure at heel strike [48]. Additionally, in the simulation, a 200-W dc brushless motor (Maxon EC-Powermax 30) is assumed, with rotor inertia $I_m = 30.4\,\mathrm{g/cm^2}$. Motor damping b_e is set equal to 8,250 Ns/m based on experimental measurements in [31]. Furthermore, a ballscrew transmission (Nook ECN-10030-LG, 10 mm × 3 mm) is assumed ($R = 3{,}560$), specifically sized for a nominal male foot size of 27 cm, with a maximum transmission load rating of 5 kN. Thus, the design goal is to select a series spring constant such that the peak shock load applied to the transmission is equal to or less than the maximum transmission load rating of 5 kN.

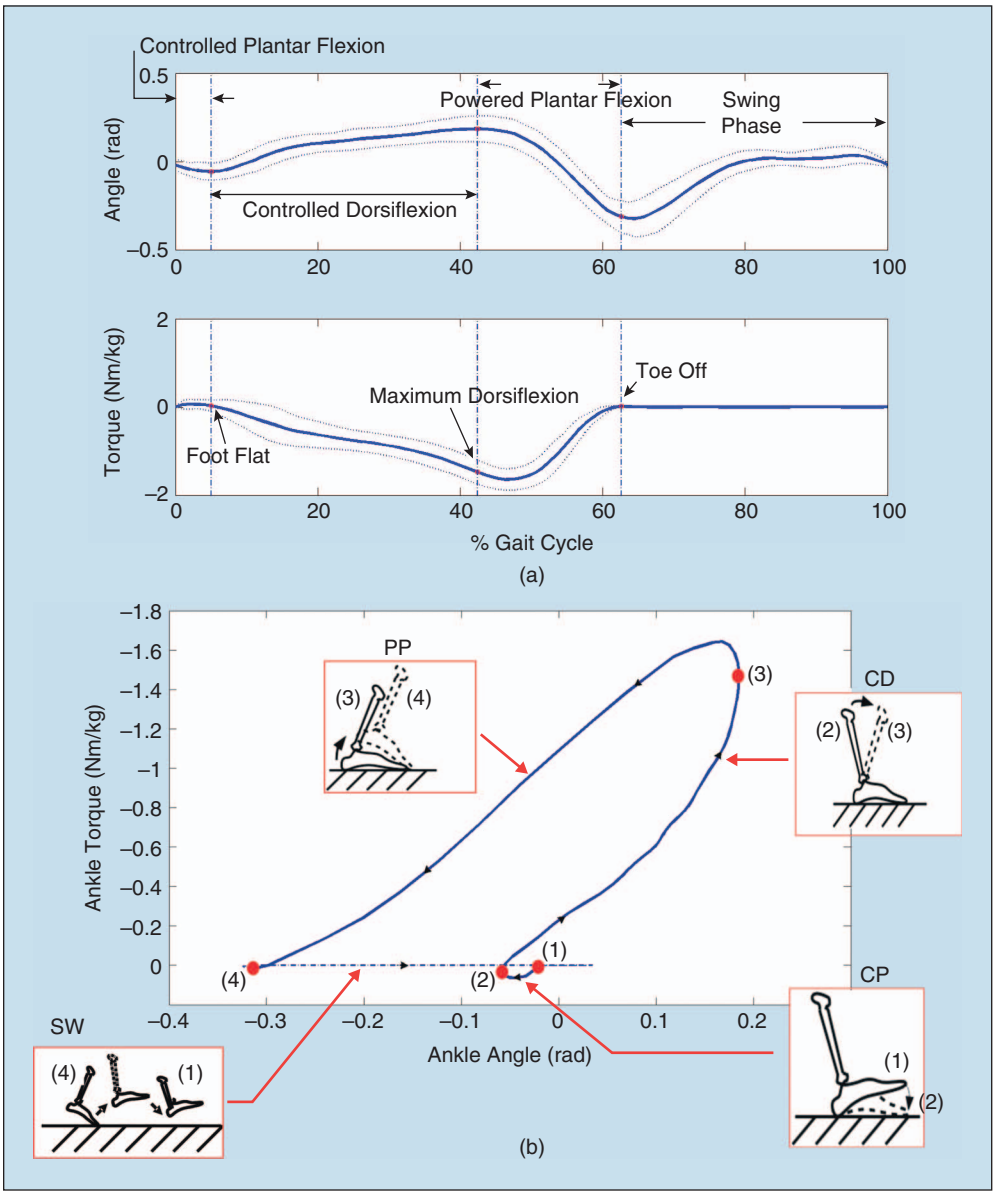

Figure 1. *Human ankle kinematics and kinetics at a self-selected walking speed [9]. (a) Average ankle angle and torque data for 16 study participants are plotted versus percent gait cycle. The dotted lines represent the first standard deviations of the ankle angle and torque data over one gait cycle. One complete walking cycle is shown [from heel strike (0%) to heel strike (100%) of the same leg]. (b) Ankle torque is plotted versus ankle angle. The solid line shows the ankle torque-angle behavior during stance, whereas the dashed line shows the swing phase. Points (1), (2), (3), and (4) denote the gait events of heel strike, foot flat, maximum dorsiflexion, and toe off, respectively. The segments (1)–(2), (2)–(3), (3)–(4), and (4)–(1) represent the ankle torque-angle behaviors during gait phases of controlled plantar flexion (indicated by CP), controlled dorsiflexion (indicated by CD), powered plantar flexion (indicated by PP), and swing phase (indicated by SW), respectively. The area enclosed by points (1), (2), (3), and (4) is the net work done at the joint during stance (or 0.21 J/kg).*

The results are plotted in Figure 3. The gray region indicates the estimated peak shock load applied to the transmission for different series spring constants under different active motor impedances. The

upper boundary denotes the peak load when the motor shaft is held fixed or when linear motor force F_e of (1) is sufficiently large to hold the effective mass M_e at a fixed position. In distinction, the lower boundary is simulated under the condition that the motor moves freely with F_e equal to zero. From Figure 3, we see that a series stiffness value of 600 kN/m results in a peak transmission force approximately equal to the 5-kN load limit of the ball-screw transmission.

Force Bandwidth

When designing a controller, one needs to guarantee that the actuator system does not saturate within the desired operating range of torque and speed. A critical actuator performance metric is the open-loop force bandwidth. As highlighted in the previous section, series compliance improves shock tolerance by limiting shock loads applied to the transmission. However, this advantage comes with a price. Although shock tolerance is improved, because of motor saturation, the open-loop force bandwidth is reduced when a spring is placed in series with the motor and transmission. Thus, when designing a motorized ankle-foot prosthesis, series spring stiffness has to be carefully selected so as to provide adequate actuator shock tolerance and force bandwidth.

In the section "Biomimetic Design Goals," a 17-Hz open-loop torque bandwidth was specified as the lower limit to still allow a prosthetic controller to capture the torque-velocity behavior of the human ankle in walking. For a prosthetic ankle-foot device, what series compliance is necessary to produce at least that bandwidth? To answer this question, we set the ankle angle θ equal to zero, making the equation of motion (1) for this model equivalent to a standard second-order differential equation for a spring-mass-damper system.

With the series spring force F_s considered as the system output, the transfer function that describes the force bandwidth due to the maximum input motor force F_{sat} is

$$\frac{F_s^{\max}}{F_{\text{sat}}} = \frac{k_s}{M_e s^2 + (b_e + \frac{F_{\text{sat}}}{V_{\text{sat}}})s + k_s}, \tag{2}$$

where $F_s^{\max}$ and V_{sat} are the maximum output spring force and linear velocity, respectively. An additional linear damping term, $F_{\text{sat}}/V_{\text{sat}}$, was included in (2) to model the effect of back-electromotive force (EMF) to the motor [42]. This term describes the inability of the amplifier to produce high force (or a loss in motor force) because of the back-emf of the motor. We set $F_{\text{sat}} = RT_{\text{motor}}^{\max}$ and $V_{\text{sat}} = \omega^{\max}/R$, where $T_{\text{motor}}^{\max}$ and $\omega^{\max}$ are the stall torque and maximum angular velocity of the motor, respectively. As can be seen in (2), the

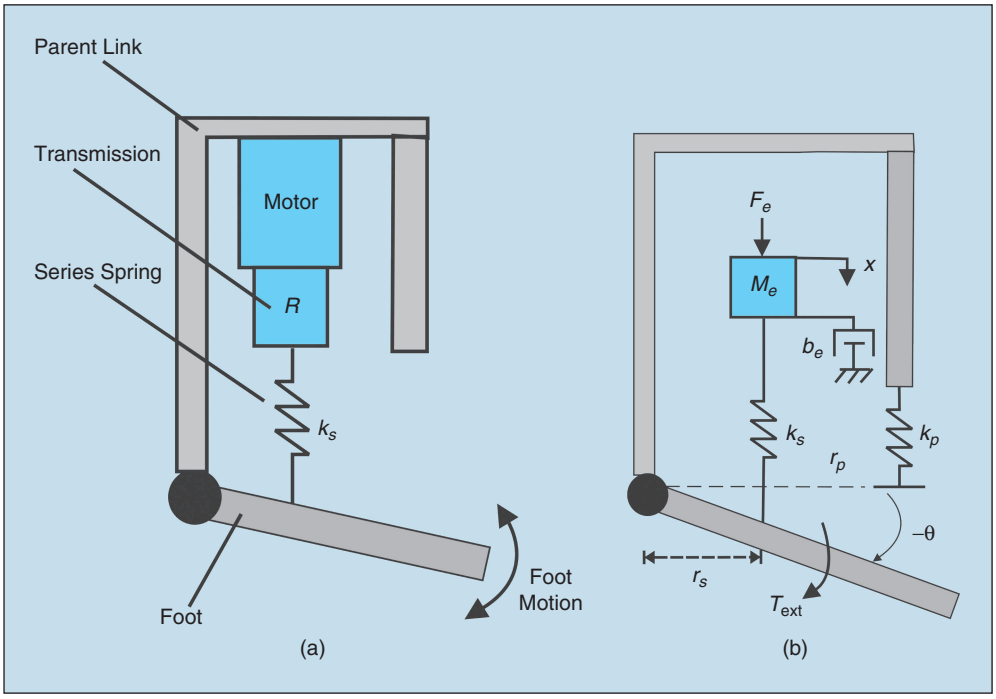

Figure 2. *A powered prosthesis with series elasticity: (a) schematic model and (b) linear model.*

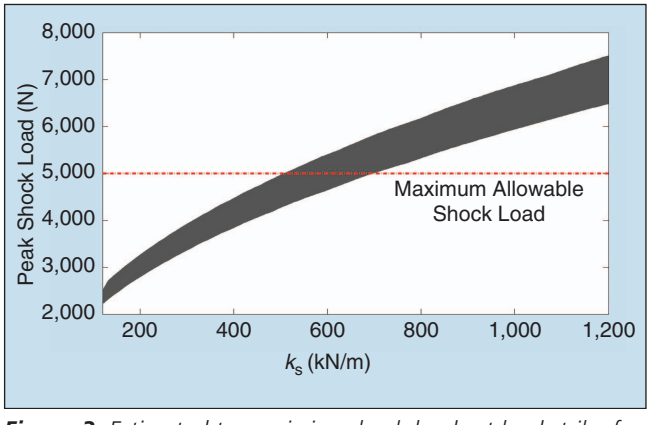

Figure 3. *Estimated transmission shock loads at heel strike for different series spring stiffnesses and active motor impedance levels.*

Table 1. Design specifications for a nominal male subject.

Total prosthetic mass (kg)	2.0
Peak torque (Nm)	125.0
Peak velocity (rad/s)	3.6
Peak power (W)	234.0
Open-loop torque bandwidth (Hz)	17.0
Net work done (J)	16.0
Controlled dorsiflexion stiffness (Nm/rad)	630.0

open-loop bandwidth depends on the intrinsic system behavior determined by the motor, transmission, and series spring. Using the same motor (EC-Powermax 30) and ball-screw transmission ($R = 3{,}560$) employed in the shock tolerance simulations of the previous section, the bandwidth simulation results are plotted in Figure 4. At the peak actuator force (horizontal line at $F_s^{\max}/F_{\text{sat}} = 0.18$), the force bandwidth for three distinct series motor spring stiffnesses, or 120, 600, and 1,200 kN/m, is 0.8, 4, and 8 Hz, respectively. Thus, the greatest series stiffness that offers adequate shock tolerance, or 600 kN/m, fails to provide sufficient bandwidth (bandwidth specification of 17 Hz, see Table 1).

As a resolution to this difficulty, we introduce parallel motor elasticity to the prosthetic architecture. As shown in Figure 5, the parallel spring is unidirectional, meaning that the spring engages only for ankle angles less than zero degrees (ankle dorsiflexed). Parallel elasticity increases the open-loop force bandwidth because force levels borne by the SEA are effectively lowered. By setting the parallel spring stiffness equal to the human-controlled dorsiflexion stiffness (see Table 1, $K_p = 630$ Nm/rad), the peak SEA force becomes $F_s^{\max}/F_{\text{sat}} = 0.023$, increasing the bandwidth to 20 Hz (see Figure 4).

In summary, the maximum level of series stiffness that adequately protects the transmission from damage during heel strike fails to satisfy bandwidth requirements. As a resolution to this difficulty, parallel motor elasticity is used to lower the forces borne by the SEA, increasing force bandwidth to an acceptable level for biomimetic ankle-foot behavior.

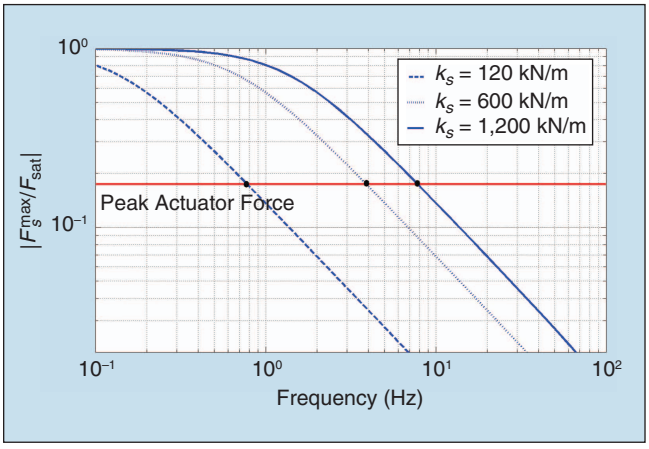

Figure 4. *Force bandwidth due to motor saturation.*

Energy Economy

A powered prosthesis must operate for at least one full day on a single battery charge. Prosthesis energy economy is therefore of critical importance, especially when one considers the requirement that the prosthesis must be lightweight. We define energy economy as an energetic cost of transport (COT) or the electrical energy required to transport unit body weight (amputee + prosthesis) in unit distance. We normalize the electrical energy consumption by body weight times distance traveled given the fact that a greater amount of ankle net work, and therefore a greater amount of electrical energy to pay for that net work, is required to transport a heavier amputee.

What are the stiffness values for the series and parallel springs that minimize prosthesis COT? To answer this question, we use a standard dc motor model to estimate the electrical energy consumption of the prosthesis. The equations are as follows:

$$I = I_{nl}\text{sgn}(\dot{\theta}_m) + \frac{T_m}{K_t}, \quad (3)$$

$$V = \frac{\dot{\theta}_m}{K_e} + R_m I, \quad (4)$$

$$P_m = IV, \quad (5)$$

where I, V, and P_m are the motor current, voltage, and electrical power consumption, respectively. Furthermore, K_e, K_t, I_{nl}, and R_m are the speed constant, torque constant, no load current, and motor resistance, respectively.

Using the reference human ankle angle and torque trajectories in Figure 1(a), we estimate the required linear motor movement and its derivatives $(x, \dot{x}, \ddot{x})$ and also the required motor torque T_m. We then

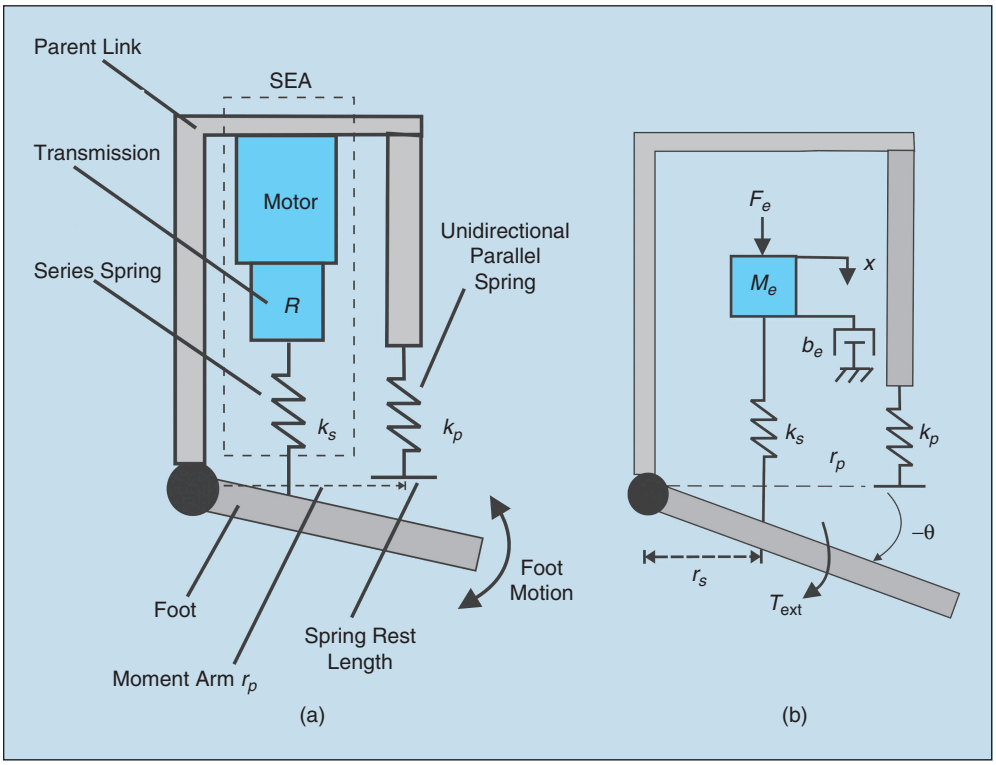

Figure 5. *A powered prosthesis with both series and parallel elasticity: (a) schematic model and (b) linear model.*

compute the electrical motor power consumption using (3)–(5) and obtain the electrical energy consumption of the motor by integrating electrical power (5) over one gait cycle. When computing energy consumption, we assume that only 30% of the negative electrical energy can be stored and reused to provide the energy for ankle-powered plantar flexion. Figure 6 shows the simulation results of the prosthesis COT for different total reduction ratios and stiffness values of series and parallel springs. Parallel stiffness, normalized by the human-controlled dorsiflexion stiffness of 630 Nm/rad (see Table 1), is noted as $\hat{K}_p$ on the upper portion of each graph. Without parallel stiffness ($\hat{K}_p = 0$), the energy consumption of the prosthesis is minimal at a total reduction ratio greater than 400 and a series spring stiffness greater than 400 kN/m. As parallel spring stiffness increases ($\hat{K}_p > 0$), the prosthesis COT can attain a lower minimum value while also requiring a smaller total reduction ratio and series spring stiffness. Using a lower reduction ratio allows the system to have a larger bandwidth and a faster intermittent response.

Using step-count monitoring systems, researchers have determined that active transtibial amputees walk 3,060 ± 1,890 steps per day [49]. Assuming the case of a nominal male amputee walking for 5,000 steps at a moderate walking speed, how large would the onboard battery have to be? Using a parallel spring stiffness equal to the human ankle stiffness ($\hat{K}_p = 1$), and the shock-tolerant series stiffness of 600 kN/m, the optimized prosthesis COT is 0.05 (see Figure 6) at an optimal total reduction ratio greater than, or equal to, 200. For a nominal male of 78 kg walking at a self-selected speed of 1.25 m/s, with a cycle time of 1.1 s (see Figure 1), this COT value converts to 26 J per walking cycle. Using a Li-Polymer battery [energy density 165 W/h/kg (e.g., www.thunderpowerrc.com)], a 0.22-kg battery would enable 5,000 steps of powered walking. This battery mass is reasonable as it is the same size as the required battery for the Össur's Proprio Foot [8] now being sold commercially.

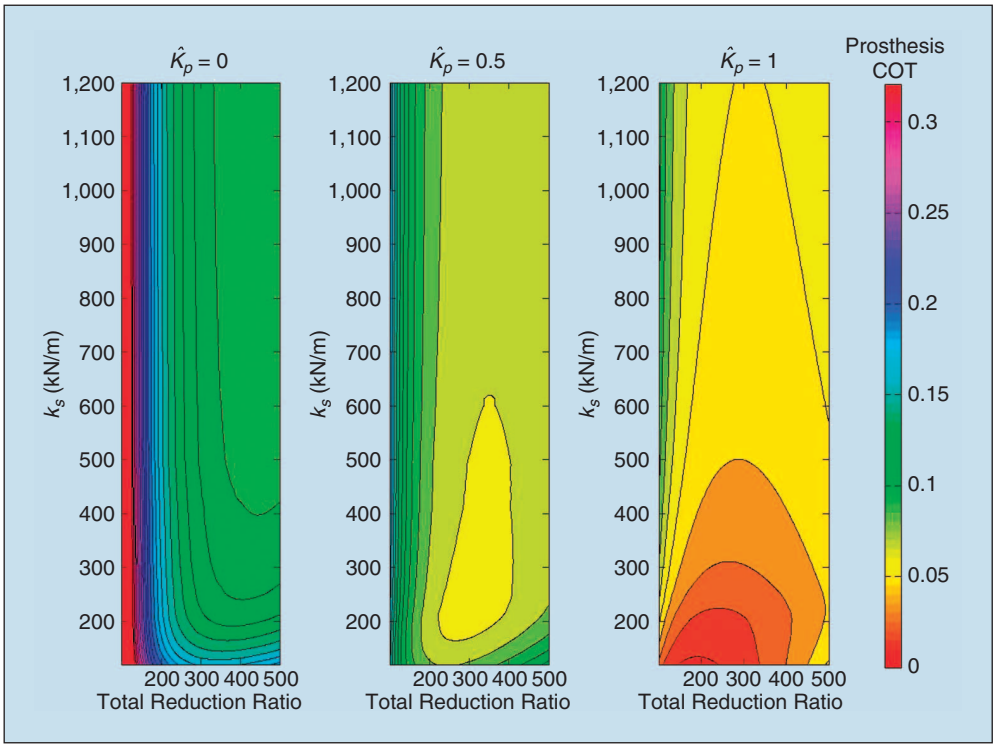

Figure 6. *The effect of total reduction ratio, series stiffness, and parallel stiffness on prosthesis COT. The total reduction ratio is equal to the SEA moment arm r multiplied by transmission ratio R. The prosthesis COT is equal to the amount of electrical energy consumed in one walking cycle divided by half body weight (0.5 × 78 kg × 9.8 m/s^2) and the distance traveled during one walking cycle (1.25 m/s × 1.1 s cycle time = 1.4 m).*

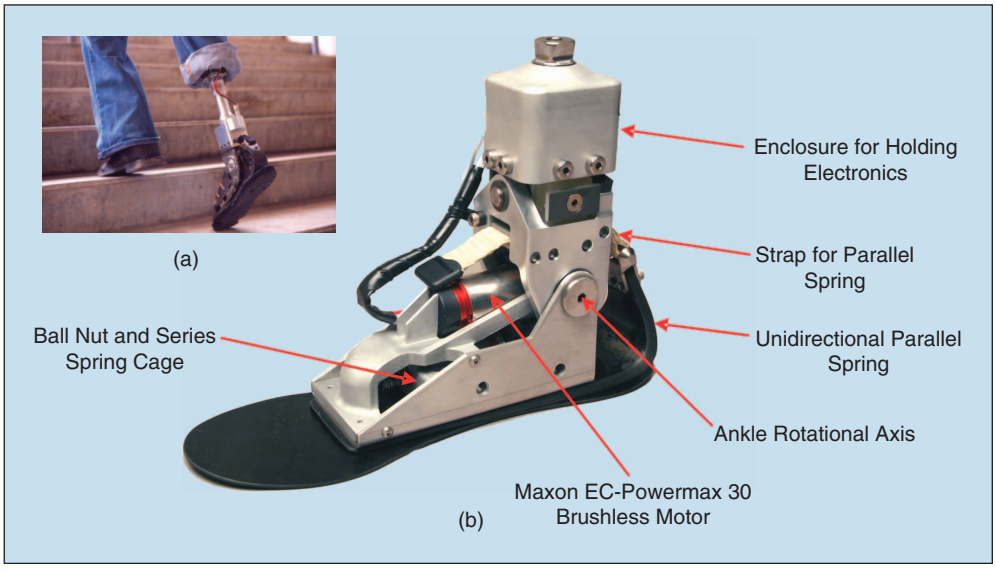

Figure 7. *Powered ankle-foot prosthesis with series and parallel elasticity. (a) The prosthesis is shown powering an amputee up a flight of stairs. (b) The powered prosthesis is shown including all components except for the battery.*

Prosthesis Implementation and Assessment

The ankle-foot prosthesis is shown in Figure 7. The prosthesis weighs 2 kg, which includes a 0.22-Kg battery. The battery attaches to the prosthetic socket (not shown in Figure 7). The unidirectional parallel spring is a leaf spring made from carbon composite material, having a rotary stiffness of 630 Nm/rad. The series spring is formed by polyurethane material positioned in series with a ball-screw transmission (Nook ECN-10030-LG, 10 mm $\times$ 3 mm), having a linear stiffness of 600 kN/m. The total reduction ratio is 170. The EC-Powermax 30 motor from Maxon was selected because of its small size and weight. Although the control system design for the prosthesis is not described here, an interested reader can see [34], [35].

During system evaluations, we found that for a 76-kg walking transtibial amputee, the powered ankle-foot prosthesis delivered a peak ankle velocity, torque, and power equal to 2.1 $\pm$ 0.1 rad/s, 141 $\pm$ 2 Nm, and 230 $\pm$ 10 W, respectively ($N = 8$ walking trials at 1.3 m/s). Furthermore, the powered prosthesis provided a net positive stance work and controlled dorsiflexion stiffness of 12.6 $\pm$ 0.2 J and 576 $\pm$ 5 Nm/rad, respectively. These prosthetic values agree reasonably well with the target human ankle values listed earlier in the section "Biomimetic Design Goals." Furthermore, the prosthesis required 30 J per step of electrical energy at a 1.3 m/s walking speed and a cycle distance equal to 1.4 m. Thus, the prosthesis COT was 0.06, similar to the predicted value in Figure 6.

The prosthesis is shown to deliver similar ankle dynamics in walking compared with a biological ankle, but does it have the capability to improve amputee gait? In a preliminary investigation on the clinical efficacy of the powered prosthesis [32]–[35], we measured the rate of oxygen consumption and carbon dioxide production as a determinant of metabolic rate on three unilateral transtibial amputees walking at self-selected speeds. With only a modest accommodation period of approximately two hours, we found that the powered prosthesis improved amputee metabolic economy on average by 14% compared with the conventional passive-elastic prostheses evaluated (Flex-Foot Ceterus and Freedom Innovations Sierra), highlighting the clinical importance of prosthetic interventions that closely mimic the mass distribution, kinetics, and kinematics of the missing limb. [Metabolic economy is defined as the amount of metabolic energy required to transport unit amputee weight (unit distance). For a detailed experimental methodology, see [32]–[35].]

Conclusions

The minimum level of series compliance that adequately protects the transmission from damage during foot collision fails to satisfy bandwidth requirements. As a resolution to this difficulty, parallel motor elasticity is used to lower the forces borne by the SEA, enhancing system force bandwidth. To minimize prosthesis COT and motor or transmission size, we select a parallel stiffness that supplies the necessary ankle stiffness during early stance period dorsiflexion, eliminating the need for SEA during that gait phase. In future investigations, we hope to apply the ankle-foot design to robotic, orthotic, and exoskeletal applications. In the design of biomimetic ankle-foot systems, we feel both series and parallel motor elasticity are of paramount importance.

Acknowledgments

This research was supported by the U.S. Veterans Administration under grant VA241-P-0026 and by the Army Telemedicine and Advanced Technology Division under grant W81XWH-07-1-0343. We would like to acknowledge the contributions of Manta Designs and Massachusetts Institute of Technology (MIT) researchers Chris Barnhart, Bruce Deffenbaugh, and Jeff Weber for their invaluable electromechanical design work.

Keywords

Powered ankle-foot prosthesis, amputee gait, series elasticity, parallel elasticity, impedance control.

References

[1] N. H. Molen, "Energy/speed relation of below-knee amputees walking on motor-driven treadmill," *Eur. J. Appl. Physiol.*, vol. 31, no. 3, pp. 173–185, 1973.

[2] E. G. Gonzalez, P. J. Corcoran, and R. L. Reyes, "Energy expenditure in B/K amputees: Correlation with stump length," *Arch. Phys. Med. Rehabil.*, vol. 55, no. 3, pp. 111–119, 1974.

[3] G. R. Colborne, S. Naumann, P. E. Longmuir, and D. Berbrayer, "Analysis of mechanical and metabolic factors in the gait of congenital below knee amputees: A comparison of the SACH and Seattle Feet," *Am. J. Phys. Med. Rehabil.*, vol. 71, no. 5, pp. 272–278, 1992.

[4] D. J. Sanderson and P. E. Martin, "Lower extremity kinematic and kinetic adaptations in unilateral below-knee amputees during walking," *Gait Posture*, vol. 6, no. 2, pp. 126–136, 1997.

[5] A. Esquenazi and R. DiGiacomo, "Rehabilitation after amputation," *J. Am. Podiatr. Med. Assoc.*, vol. 91, no. 1, pp. 13–22, 2001.

[6] L. Torburn, C. M. Powers, R. Guiterrez, and J. Perry, "Energy expenditure during ambulation in dysvascular and traumatic below-knee amputees: A comparison of five prosthetic feet," *J. Rehabil. Res. Dev.*, vol. 32, no. 2, pp. 111–119, 1995.

[7] M. J. Hsu, D. H. Nielsen, S.-J. L. Chan, and D. Shurr, "The effects of prosthetic foot design on physiologic measurements, self-selected walking velocity, and physical activity in people with transtibial amputation," *Arch. Phys. Med. Rehabil.*, vol. 87, no. 1, pp. 123–129, 2006.

[8] Össur, Inc. (2008). [Online]. Available: www.ossur.com

[9] S. Ron, *Prosthetics and Orthotics: Lower Limb and Spinal*. Baltimore, MD: Lippincott Williams & Wilkins, 2002.

[10] A. L. Hof, B. A. Geelen, and J. W. Van Den Berg, "Calf muscle moment, work and efficiency in level walking; role of series elasticity," *J. Biomech.*, vol. 16, no. 7, pp. 523–537, 1983.

[11] D. A. Winter, "Biomechanical motor pattern in normal walking," *J. Mot. Behav.*, vol. 15, no. 4, pp. 302–330, 1983.

[12] M. Palmer, "Sagittal plane characterization of normal human ankle function across a range of walking gait speeds," M.S. thesis, Dept. Mech. Eng., MIT, Cambridge, MA, 2002.

[13] D. H. Gates, "Characterizing ankle function during stair ascent, descent, and level walking for ankle prosthesis and orthosis design," M.S. thesis, Dept. Biomed. Eng., Boston Univ., MA, 2004.

[14] A. Hansen, D. Childress, S. Miff, S. Gard, and K. Mesplay, "The human ankle during walking: Implication for the design of biomimetric ankle prosthesis," *J. Biomech.*, vol. 37, no. 10, pp. 1467–1474, 2004.

[15] D. A. Winter and S. E. Sienko, "Biomechanics of below-knee amputee gait," *J. Biomech.*, vol. 21, no. 5, pp. 361–367, 1988.

[16] A. D. Kuo, "Energetics of actively powered locomotion using the simplest walking model," *J. Biomech. Eng.*, vol. 124, no. 1, pp. 113–120, 2002.

[17] A. D. Kuo, J. M. Donelan, and A. Ruina, "Energetic consequences of walking like an inverted pendulum: Step-to-step transitions," *Exerc. Sport Sci. Rev.*, vol. 33, no. 2, pp. 88–97, 2005.

[18] A. Ruina, J. E. Bertram, and M. Srinivasan, "A collisional model of the energetic cost of support work qualitatively explains leg sequencing in

walking and galloping, pseudo-elastic leg behavior in running and the walk-to-run transition," *J. Theor. Biol.*, vol. 237, no. 2, pp. 170–192, 2005.
[19] K. Koganezawa and I. Kato, "Control aspects of artificial leg," in *Proc. IFAC Symp. Control Aspects of Biomedical Engineering*, 1987, pp. 71–85.
[20] S. Au, P. Dilworth, and H. Herr, "An ankle-foot emulation system for the study of human walking biomechanics," in *Proc. IEEE Int. Conf. Robotics and Automation*, Orlando, FL, May 2006, pp. 2939–2945.
[21] K. Hirai, M. Hirose, Y. Haikawa, and T. Takenaka, "The development of Honda humanoid robot," in *Proc. IEEE/RSJ Int. Conf. Intelligent Robots and Systems*, Leuven, Belgium, May 1998, pp. 1321–1326.
[22] K. Kaneko, F. Kanehiro, S. Kajita, H. Hirukawa, T. Kawasaki, M. Hirata, K. Akachi, and T. Isozumi, "Humanoid robot HRP-2," in *Proc. IEEE Int. Conf. Robotics and Automation*, New Orleans, LA, April 2004, pp. 1083–1090.
[23] "Self-adjusting prosthetic ankle apparatus," U.S. Patent 6 443 993, Sept. 3, 2002.
[24] S. H. Collins and A. D. Kuo, "Controlled energy storage and return prosthesis reduces metabolic cost of walking," in *Proc. ISB 20th Congr. and the American Society of Biomechanics Annu. Meeting*, Cleveland, Ohio, 2003, p. 804.
[25] C. Li, M. Tokuda, J. Furusho, K. Koyanagi, S. Morimoto, Y. Hashimoto, A. Nakagawa, and Y. Akazawa, "Research and development of the intelligently controlled prosthetic ankle joint," in *Proc. IEEE Int. Conf. Mechatronics and Automation*, Luoyang, China, 2006, pp. 1114–1119.
[26] A. H. Hansen, S. A. Gard, D. S. Childress, B. Ruhe, and R. Williams, "Automatically adapting ankle-foot prosthesis concept," in *12th World Congr. Int. Society for Prosthetics and Orthotics*, Vancouver, Canada, 2007.
[27] G. K. Klute, J. Czerniecki, and B. Hannaford, "Development of powered prosthetic lower limb," in *Proc. 1st Nat. Meeting, Veterans Affairs Rehabilitation R&D Service*, Washington, DC, Oct. 1998.
[28] H. Herr, D. Paluska, P. Dilworth, and S. Kwau, "A hybrid actuator comprising motor, spring and variable-damper elements," Patent Provisional F-51 SN 60/666,876, Mar. 31, 2005.
[29] S. Au, P. Bonato, and H. Herr, "An EMG-position controlled system for an active ankle-foot prosthesis: An initial experimental study," in *Proc. IEEE 9th Int. Conf. Rehabilitation Robotics (ICORR)*, Chicago, IL, June 2005, pp. 375–379.
[30] S. Au and H. Herr, "Initial experimental study on dynamic interaction between an amputee and a powered ankle-foot prosthesis," presented at the Workshop on Dynamic Walking: Mechanics and Control of Human and Robot Locomotion, Ann Arbor, MI, May 2006.
[31] S. K. Au, J. Weber, and H. Herr, "Biomechanical design of a powered ankle-foot prosthesis," in *Proc. IEEE Int. Conf. Rehabilitation Robotics*, Noordwijk, The Netherlands, June 2007, pp. 298–303.
[32] S. Au, J. Weber, E. Martinez-Villapando, and H. Herr, "Powered ankle-foot prosthesis for the improvement of amputee ambulation," in *Proc. 29th Annu. Int. Conf. IEEE Engineering in Medicine and Biology Society*, Lyon, France, 2007, pp. 3020–3026.
[33] H. Herr, J. Weber, and S. Au, "Powered ankle-foot prosthesis," in *Proc. Int. Conf. Biomechanics of the Lower Limb in Health, Disease and Rehabilitation*, Manchester, England, Sept. 3–5 2007, pp. 72–74.
[34] S. K. Au, "Powered ankle-foot prosthesis for the improvement of amputee walking economy," Ph.D. dissertation, Dept. Mech. Eng., MIT, Cambridge, MA, 2007.
[35] S. Au, J. Weber, and H. Herr, "Powered ankle-foot prosthesis improves walking metabolic economy," *IEEE Trans. Robot.*, to be published.
[36] J. Hitt, R. Bellman, M. Holgate, T. Sugar, and K. Hollander, "The SPARKy (spring ankle with regenerative kinetics) projects: Design and analysis of a robotic transtibial prosthesis with regenerative kinetics," in *Proc. ASME Int. Design Engineering Tech. Conf.*, CD-ROM, 2007, pp. 1–10.
[37] D. A. Winter, *Biomechanics and Motor Control of Human Movement*, 2nd ed. New York: Wiley, 1990.
[38] V. T. Inman, H. J. Ralston, and F. Todd, *Human Walking*. Baltimore: Williams and Wilkins, 1981.
[39] J. Perry, *Gait Analysis: Normal and Pathological Function*. Thorofare, New Jersey: SLACK Inc., 1992.
[40] A. R. Tilley, H. Dreyfuss, and S. B. Wilcox, *The Measure of Man and Woman: Human Factors in Design*, rev. ed. New York: Wiley, 2001.
[41] G. A. Pratt and M. M. Williamson, "Series elastic actuators," in *Proc. IEEE/RSJ Int. Conf. on Intelligent Robots and Systems*, Pittsburgh, 1995, pp. 399–406.
[42] D. Robinson, "Design and an analysis of series elasticity in closedloop actuator force control," Ph.D. dissertation, Dept. Mech. Eng., MIT, Cambridge, MA, 2000.
[43] J. Pratt, A. Torres, P. Dilworth, and G. Pratt, "Virtual actuator control," in *Proc. IEEE Int. Conf. Intelligent Robots and Systems (IROS '96)*, Osaka, Japan, 1996, pp. 1219–1226.
[44] J. Blaya and H. Herr, "Adaptive control of a variable-impedance ankle-foot orthosis to assist drop foot gait," *IEEE Trans. Neural. Syst. Rehabil. Eng.*, vol. 12, no. 1, pp. 24–31, 2004.
[45] C. Walsh, K. Pasch, and H. Herr, "An autonomous, underactuated exoskeleton for load-carrying augmentation," in *Proc. IEEE/RSJ Int. Conf. Intelligent Robots and Systems (IROS)*, Beijing, China, October 9–16, 2006, pp. 1410–1415.
[46] C. Walsh, D. Paluska, K. Pasch, W. Grand, A. Valiente, and H. Herr, "Development of a lightweight, underactuated exoskeleton for load-carrying augmentation," in *Proc. IEEE Int. Conf. Robotics and Automation*, Orlando, FL, May 2006, pp. 2939–2945.
[47] J. M. Donelan, R. Kram, and A. D. Kuo, "Simultaneous positive and negative external mechanical work in human walking," *J. Biomech.*, vol. 35, no. 1, pp. 117–124, 2002.
[48] M. Popovic, A. Goswami, and H. Herr, "Ground reference points in legged locomotion: Definitions, biological trajectories and control implications," *Int. J. Robot Res.*, vol. 24, no. 12, pp. 1013–1032, 2005.
[49] J. M. Stepien, S. Cavenett, L. Taylor, and M. Crotty, "Activity levels among lower-limb amputees: Self-report versus step activity monitor," *Arch. Phys. Med. Rehabil.*, vol. 88, no. 7, pp. 896–900, 2007.

Samuel K. Au received his B.S. and M.S. degrees from the Department of Automation and Computer-Aided Engineering at the Chinese University of Hong Kong and his Ph.D. degree from the Mechanical Engineering Department at MIT. He is currently a postdoctoral associate working in the Biomechatronics Group within the MIT Media Lab. His research interests include system dynamics, system identification, biomedical signal processing, control, biomechanics, artificial intelligence, robotics, and prosthetics.

Hugh M. Herr received the B.A. degree in physics from the Millersville University of Pennsylvania in 1990, the M.S. degree in mechanical engineering from MIT, and the Ph.D. degree in biophysics from Harvard University in 1998. He is an associate professor within MIT's Program of Media Arts and Sciences and the Harvard-MIT Division of Health Sciences and Technology. His primary research objective is to apply the principles of biomechanics and neural control to guide the designs of prostheses, orthoses, and exoskeletons. He is the author of more than 60 technical publications in biomechanics and wearable robotics and is an active Member of the IEEE. He is the recipient of the 2007 Heinz Award for Technology, the Economy, and Employment.

Address for Correspondence: Hugh M. Herr, Biomechatronics Group, MIT Media Lab, E15-424, Cambridge, MA 02139, USA. E-mail: hherr@media.mit.edu.